Peter Johansen*
Bioengineering Department,
Penn State University,
University Park, PA 16802,
Department of Cardiothoracic
and Vascular Surgery,
Aarhus University Hospital Skejby Sygehus,
8200 Aarhus N., Denmark

Keefe B. Manning
Bioengineering Department,
Penn State University,
University Park, PA 16802

John M. Tarbell
Department of Biomedical Engineering,
The City College of New York (CUNY)
,New York, NY 10031

Arnold A. Fontaine

Steven Deutsch

Applied Research Laboratory,
Penn State University,
University Park, PA 16802

Hans Nygaard
Department of Cardiothoracic
and Vascular Surgery,
Aarhus University Hospital Skejby Sygehus,
8200 Aarhus N., Denmark

A New Method for Evaluation of Cavitation Near Mechanical Heart Valves

Evaluation of cavitation in vivo is often based on recordings of high-pass filtered random high-frequency pressure fluctuations. We hypothesized that cavitation signal components are more appropriately assessed by a new method for extraction of random signal components of the pressure signals. We investigated three different valve types and found a high correlation between the two methods (r^2:0.8806−0.9887). The new method showed that the cavitation signal could be extracted without a priori knowledge needed for setting the high-pass filter cut off frequency, nor did it introduce bandwidth limitation of the cavitation signal. [DOI: 10.1115/1.1613297]

Background

Patients with heart-valve dysfunction are most often treated surgically with implantation of mechanical heart-valve prostheses. Currently, over 175,000 heart valves are implanted in the world each year [1]. Although this mostly is a life-saving procedure, patients with these prostheses face potential complications. The most common of these complications are thromboembolic and bleeding disorders, but material damage of mechanical heart-valve leaflets has also been observed.

Since cavitation is known to expose nearby structures to strong erosive forces [2], this phenomenon has been suggested as a possible contributor to the thromboembolic complications and material failures [3]. Previous, evaluation of cavitation near mechanical heart valves has primarily been based on visualization of cavitation bubble formation in transparent media [4–9]. These studies have shown that cavitation bubbles can form and collapse at the inflow side of the valve immediately after its closure. These cavitation ''clouds'' have been visualized at specific locations depending on valve design, suggesting a variety of mechanisms for inception of cavitation. Since the visualization method is not applicable *in vivo*, a method using measurements of high-frequency pressure fluctuation was developed [10]. Garrison et al. recorded pressure fluctuations at beats with and without cavitation. They found that beats with no cavitation had no frequency components above 35 kHz, whereas beats with cavitation had higher frequency components. Mechanical resonance generated by the closure of the mechanical heart valve was found to have frequency components up to 35 kHz. By removing these components through a high-pass (HP) filter, Garrison et al. isolated the cavitation signal. The root mean square (RMS) value of the high-pass filtered data was calculated, and its magnitude correlated well with the degree of cavitation observed visually.

However, when applying this technique, appropriate selection of the HP filter cutoff frequency should be based on knowledge of the individual valve's closing sound characteristics [11]. Furthermore, since there may be a frequency overlap between valve closure resonance and cavitation signal components, this method might remove components from the cavitation signal.

Consequently, using this method in vivo either during animal experiments or carrying out a clinical patient-related protocol may cause difficulties in choosing the right parameters needed for setting up the analysis. A method which requires no *a priori* knowledge is desired. Therefore, a slight different approach could be utilized. The cavitation signals recorded using pressure transducers or hydrophones are caused by the momentary large pressures generated when the contents of a collapsing bubble become highly compressed [12]. The resonance frequency of a bubble is related to the bubble radius, such that smaller bubbles have higher reso-

*Corresponding address: Department of Cardiothoracic and Vascular Surgery, Aarhus University Hospital Skejby Sygehus, Brendstrupgaardsvej, 8200 Aarhus N., Denmark. Phone: +45 8949 5486; Fax: +45 8949 6016; e-mail: peter.johansen@iekf.au.dk.

Contributed by the Bioengineering Division for publication in the JOURNAL OF BIOMECHANICAL ENGINEERING. Manuscript received by the Bioengineering Division November 14, 2002; revision received April 17, 2003. Associate Editor: A. Yoganathan.

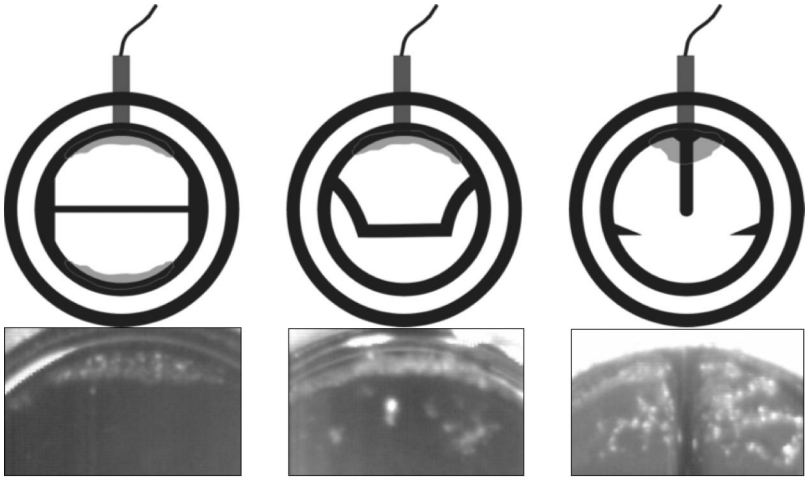

Fig. 1 The top three schematics of the investigated valves show areas (shaded) of highest probability to find cavitation. The transducer position is illustrated as the dark shaded rectangle on the atrial aspect with the wire leaving. Below the schematics are three photographs which visualizes the cavitation.

nance peak frequencies than larger bubbles. Cavitation formations that have been observed near mechanical heart valves contained numerous single cavities, each having its own frequency spectrum. This variation in bubble size perhaps creates the broad-banded frequency signature of the pressure signal observed. Since there is also beat-to-beat variation in the number and size of bubbles, it can be assumed that the sound generated exhibits randomness in the form of a non-deterministic frequency pattern. The work of Oba et al., which found stochastic behavior of desinent cavitation supports this theory [13].

Hypothesis

Separation of cavitation and valve closure signal components can be accomplished by separation of deterministic and non-deterministic components without *a priori* knowledge of valve closure resonance.

Aim of Study

To develop an alternative signal analysis method than high-pass filtering, for the separation of cavitation from valve closing sounds. The new method must be applicable to different valve types.

Material and Methods

Three different 29 mm mitral valves with an intact suture ring were investigated: The Björk-Shiley monostrut, the Medtronic Hall, and the CarboMedics CPHV standard mitral bileaflet valve. They were operated in a custom-made single-shot valve-closing model similar to the one described by Kini et al. [14] and Chandran and Aluri [15]. The model was manufactured from acrylic for optical access. It encompassed two chambers. The smaller ventricular chamber was sealed and connected to a pneumatic pressure regulator system (Air compressor pulsatile pump, Vitamek Inc., Houston, TX). The larger atrial chamber was held open to the atmosphere in order to provide a stable hydrostatic pressure to simulate ventricular preload. A transparent blood analog fluid consisted of 40% glycerin and 60% water to mimic blood's viscosity and density ($\mu = 3.5$ cP, $\rho = 1.1$ g/cm^3). The tap water used was filtered and stored for degasing for at least 24 hours. The mixed solution was also set to degas for at least 24 hours.

A high-speed video camera system (Kodak Motion Corder Analyzer, RedLake MASD, San Diego, CA) was used to visualize the atrial side of the mitral valve with 3,000 image frames per second. A Millar™ micro tip pressure transducer was positioned in the ventricular chamber to measure the left ventricular pressure used for evaluation of dp/dt. A pressure transducer (PCB 132M30, Depew, NY, USA) positioned in the atrial chamber was used to detect high frequency pressure fluctuations (HFPF). The transducer was positioned at a skewed angle of 45°, 5 mm in front of the potential cavitation areas, which were determined prior to the experiments. Figure 1 shows the potential cavitation areas of each of the valves and the position of the pressure transducer relative to each valve in a frontal view. The shaded semi-transparent areas illustrate the potential cavitation sites for each valve. Below these drawings are frames obtained by high-speed imaging showing cavitation in these areas. The areas where cavitation was observed and location of the pressure transducer were similar to those recorded in other studies of the three investigated valves (Björk-Shiley [10], CarboMedics [16], and Medtronic Hall [9,17]).

Different loading conditions (dp/dt) were imposed by adjusting the pulsatile pump heart rate (60–170 bpm), systolic duration (20–400 ms ~5–40% of each heart cycle) and the maximum left ventricular pressure. The latter was adjusted between 120–220 mmHg and verified with a Millar catheter. Nine different loading rates were planned based on pilot experiments to allow different levels of cavitation, going from ''not visible'' to ''severe'' cavitation.

The dp/dt was assessed on a LeCroy 9310 oscilloscope (Chestnut Ridge, NY) for each adjustment prior to and after a series of recordings during one stable hemodynamic situation as described in the data analysis section.

The high-frequency pressure signal was sampled through the LeCroy 9310 oscilloscope at 2 MHz. A time segment of 1 msec of pre-triggered data was acquired followed by 4 msec of post-triggered data. The data were transferred through general purpose interface bus (GPIB) to a standard PC. A custom made program in LabVIEW (National Instruments, Austin, TX) was applied to control data transfer from the digital storage oscilloscope.

Data Analysis. For each setting of the pulsatile pump, the dp/dt was calculated according to the guidelines set by the FDA [18], as the average $\Delta P/\Delta t$ over the last 20 msec before the mitral valve closure. Hence, dp/dt was estimated as $\Delta P_{20\ msec}/20$ msec.

As an indicator of cavitation intensity, the root mean square (RMS) value of the HFPF data was calculated after it was high-

Table 1 Criteria for separating the different hemodynamic situations into various degrees of cavitation

Valve	Cavitation degree			
	None	Moderate 1	Moderate 2	High
Björk-Shiley	No visible cavitation	Formation of bubble cavitation on the disc surface. Max. duration 2/3 ms.	Formation of bubble cavitation and indication of cavitation at the edge of the leaflet. Max duration 2/3 ms.	Extensive formation of bubble cavitation and cavitation at the edge of the leaflet. Duration >2/3 ms.
CarboMedics		Formation of cavitation near leaflet edge. Max duration 2/3 ms.	Excluded	Extensive cavitation formation near leaflet edge with a duration > 2/3 ms.
Medtronic Hall		Excluded	Formation of bubble cavitation on the disc surface. Max. duration 2/3 ms.	Extensive formation of bubble cavitation and cavitation near seat stop. Duration >2/3 ms.

pass filtered using Garrison et al.'s method [10], later modified by Johansen et al. [11]. Hence, the cutoff filter matched the natural harmonic components of each valve. The cutoff frequencies chosen were for the Björk-Shiley: 40.9 kHz, CarboMedics: 53.7 kHz, and Medtronic Hall: 49.9 kHz. The high-pass filter was configured as a fifth-order Butterworth. The RMS value was calculated as:

$$RMS = \sqrt{\frac{1}{T}\int_0^T p^2(t)dt} \tag{1}$$

where T represents the data length (5 msec) and $p(t)$ is the recorded pressure data. The mean RMS value was calculated based on 30 value closures.

To isolate and quantify the non-deterministic energy as a representation of cavitation, the deterministic energy was subtracted from the total signal energy:

$$E_{\text{non-deterministic}} = E_{\text{total}} - E_{\text{deterministic}} \tag{2}$$

The $E_{\text{non-deterministic}}$ was compared with the RMS calculated from the same data, using Spearmans Rho non-parametric correlation analysis [19].

The total energy was calculated from the mean energy density spectrum of the raw data. The energy parameter was derived as:

$$E = \frac{N}{f_s} \cdot \int_0^{f_s/2} G(f) \cdot df \tag{3}$$

where N is the number of samples, f_s is the sampling frequency, and $G(f)$ is the amplitude spectrum squared. The amplitude spectrum is calculated based on discrete Fourier transformation (FTD) Eq. (4).

$$FTD: X(e^{j\omega T}) = \sum_{n=-\infty}^{\infty} x[nT] \cdot e^{-jn\omega T} \tag{4}$$

where $x[nT]$ is the input sequence, ω is the cyclic frequency and T is the time between samples. Based on this, the amplitude spectrum is the square root of the sum of the squares of the real (Re) and imaginary (Im) parts of the complex transformation result Eq. (5)

$$\text{Amplitude spectrum} |X(f)| : \sqrt{\text{Re}^2 + \text{Im}^2} \tag{5}$$

The total energy was thus calculated using equation 3 with $x[nT] = x_{\text{total}}[nT]$ being used in Eq. (4) where $x_{\text{total}}[nT]$ is the raw data input sequence of data.

The deterministic signal energy ($E_{\text{deterministic}}$) was calculated from the ensemble average of the heart cycles $x_{ea}[nT]$ using Eq. (3).

In order to line up the data in the time domain prior to ensemble averaging, a cross-correlation function was developed. First, a representative beat was chosen as a template to line up the rest of the data. The cross correlation (Rxy) between two signals ($x(t)$ and $y(t)$) for continuous data is given by

$$R_{xy}(t) = x(t) \otimes y(t) = \int_{-\infty}^{\infty} x(\tau) \cdot y(t+\tau) \cdot d\tau \tag{6}$$

where $\otimes$ denotes the cross correlation.

Considering two signals in discrete form (**X** and **Y**) where:

X has n elements, $X[j] = 0$ for $j < 0$ and $j \geqslant n$

Y has m elements, $Y[j] = 0$ for $j < 0$ and $j \geqslant m$

The cross-correlation can be implemented initially by calculation of an intermediate variable h_j:

$$h_j = \sum_{k=o}^{n-1} \sum_{j=-(n-1)}^{m-1} x_k \cdot y_{j+k} \tag{7}$$

The cross-correlation can then be calculated as:

$$R_{xyi} = h_{i-(n-1)} \tag{8}$$

Having calculated the cross-correlation, a result in the range from $0-1$ (where 1 is the highest correlation) was obtained by normalizing the result with the template chosen, (represented as $T[n]$ in digitized form), as:

$$Normalize: \frac{R_{xy}[n]}{\sum_{n=0}^{N-1} T^2[n]} \tag{9}$$

The time, τ_{ref}, where the template auto correlates with 1, is set as a reference for the line up. The maximum correlation between the template and each of the heart cycles is determined and the difference between each τ and τ_{ref} was used to adjust the temporal position of the recorded heart cycles.

Based on the high-speed visualization, each hemodynamic situation was assigned to one of three groups of cavitation intensity: none, moderate, or high. The moderate category was further divided into two sub groups. The criteria for each group are listed in Table 1.

The CarboMedics valve was expected to act with asynchronous closure, due to its bileaflet design [20]. The time between first and second leaflet closure was measured graphically by placing two cursors at the start of each leaflet closing signal.

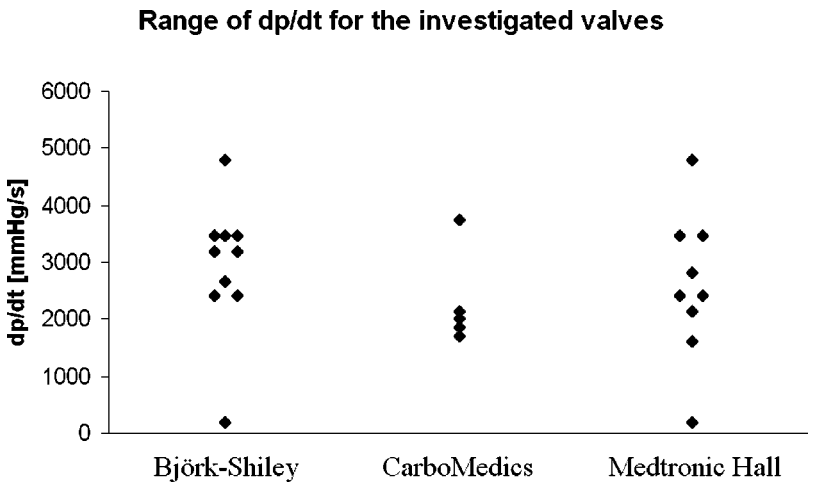

Fig. 2 The different dp/dt obtained for the different investigated valves. The mean $dp/dt \pm$ standard deviation was 2926±1183, 2286±824, and 2585 ±1296 mmHg/s for the Björk-Shiley, CarboMedics, and Medtronic Hall, respectively.

Results

Adjusting the pump settings allowed us to obtain a range of different dp/dt values for each of the three valves as illustrated in Fig. 2. The high-speed visualization data showed that the level of cavitation was a function of dp/dt. By subjectively dividing the degrees of cavitation according to the guidelines set previously (Table 1), a degree of cavitation could be assigned to each operating condition. Figure 3 depicts image frames obtained at the various degrees of cavitation. Each frame represents 1/3 ms (frame rate=3000 fps.). The degree of cavitation was also associated with the number of frames showing cavitation bubbles.

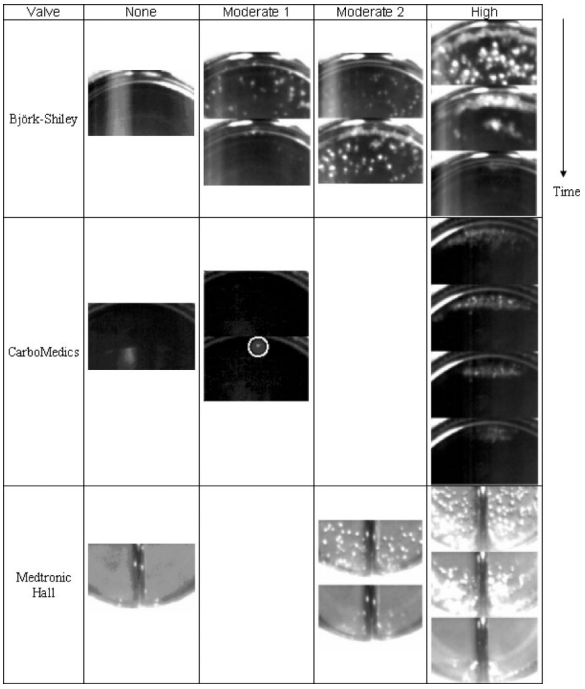

Fig. 3 Images acquired at different loading rates. The data are divided in three degrees of cavitation based on visual judgments and criteria. Only frames with visual cavitation are shown, except for the non-cavitation category. Each frame represents 1/3 msec. Successive frames are shown with time increasing downward. Contrast and brightness of the images have been adjusted to enhance details.

In processing the high-frequency pressure signal, before calculating the ensemble average, the data were temporal lined up using cross-correlation. The maximum temporal displacement of valve closures in a data series determined by the time constant τ was about 700 samples (=350 μs), which constitutes 7% of the recording window width.

Figure 4 shows an example of the spectra calculated. Both the frequency axis and the signal energy are plotted with logarithmic axes. At low frequencies and up to approximately 10 kHz most of the total signal energy is comprised of the deterministic part. At frequencies above 10 kHz the non-deterministic signal energy is about a factor 10 higher than the deterministic part.

Figure 5 shows the non-deterministic energy and dp/dt plotted as a function of the degree of cavitation based on the visual criteria (Table 1) for the three valve types. All valves show a tendency to exhibit increases in both non-deterministic energy and dp/dt as cavitation intensity increases. The Medtronic Hall valve though, has one measuring point with a lower non-deterministic energy level at higher visual cavitation level than those in the moderate cavitation degree. Furthermore, the same valve has two points in the high-cavitation-level group that are in the same range as points in the moderate-cavitation-level group.

Figure 6 shows the non-deterministic energy plotted as a function of dp/dt. The r^2 varies from 0.56−0.99 for the three valves. Both the Björk-Shiley and the CarboMedics data have a far end point. The two tilting disc had higher levels of non-deterministic energy than the bileaflet valve.

The RMS cavitation parameter is plotted as a function of the non-deterministic energy evaluated in Fig. 7. Analogous to the non-deterministic energy the RMS values were also higher for the tilting discs than the bileaflet valve. There appears to be a linear correlation between the two variables. The non-deterministic energy of the CarboMedics valve was in the range 150 −2,100 kPa^2 when visible cavitation was detected. The level increased as cavitation became more extensive spatially and temporally. The two tilting disc valves had higher ranges of non-deterministic energy than the bileaflet valve. They were 9,000 −14,000 kPa^2 (Björk-Shiley valve) and 500−16,700 kPa^2 (Medtronic Hall valve). These ranges were observed when cavitation could be visually confirmed on the high-speed video images. The dp/dt ranges for the tilting disc valves were roughly the same. Fewer measurements were taken at low dp/dt conditions

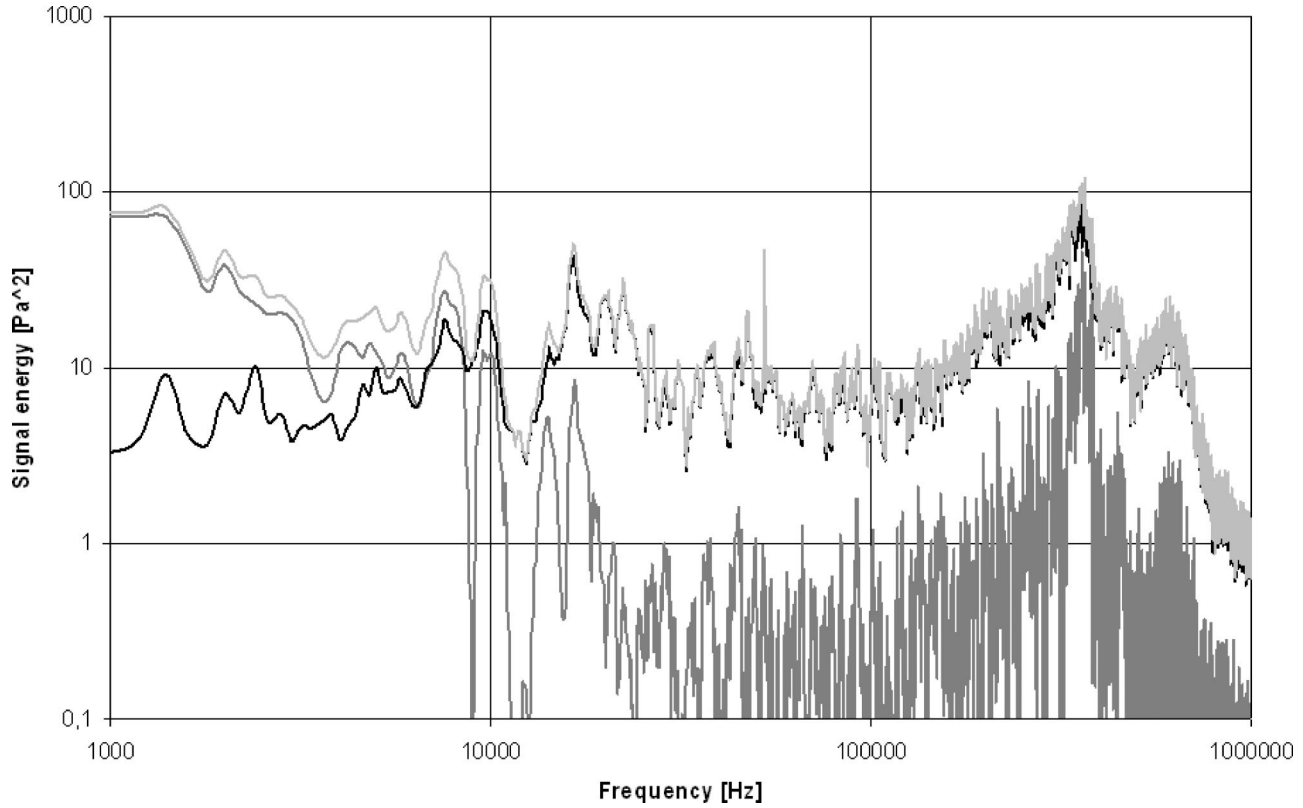

Fig. 4 The spectra calculated are the total energy spectrum, the deterministic energy spectrum calculated from the ensemble average signal, and the non-deterministic spectrum being the difference between the total and the deterministic energy spectrum. Legends Light gray: Total energy density spectrum; Dark gray: Deterministic energy density spectrum; Black: Non-deterministic energy density spectrum.

with the Medtronic Hall valve than the Björk-Shiley valve. The non-deterministic energy levels increased with increasing dp/dt. Table 2 lists the mean times and standard deviation for the duration between the two leaflet closures in the CarboMedics valve based on 40 consecutive valve closures.

Discussion

The *in vitro* model used in this study made it possible to adjust the dp/dt for different valves over a wide range. The higher values were well above the normal physiological range. These values were included to follow the severe development of cavitation and to cover a large scale of fluid dynamic situations, making the evaluation of the new method more robust. The video images showed a clear tendency of more extensive cavitation as the left ventricular pressure rate increased (Fig. 5), which is in concordance with other *in vitro* cavitation studies [21,22]. The images also showed that the first type of cavitation which could be visualized as dp/dt increased was bubbles formed on the surface of the leaflets (Fig. 3). This was observed for all the valves and indicates the onset of a ''water hammer'' type of cavitation. Higher levels of dp/dt produced ''vortex'' cavitation near the leaflet edge for the Björk-Shiley and CarboMedics valves.

With the pressure transducer positioned near the potential cavitation areas, high frequency pressure fluctuations were recorded as cavitation occurred. The extraction of the non-deterministic energy was successfully performed, and the necessity for using the cross correlation function in order to line up the data was seen, as the recorded timing of the data would vary when they were level-triggered, resulting in erroneous ensemble averaging. Even though the pressure signal was level triggered and sampled at a high acquisition rate, the heart cycles were typically displaced temporally up to 0.35 ms, which is 7% of the acquisition time window. Since it is important to make sure that data are lined up in time before performing ensemble averaging, this study presented a method to align beats using a cross correlation algorithm.

The non-deterministic energy increased when cavitation increased (Fig. 5), based on the visual determination of different cavitation degrees (Fig. 3). A semi-quantitative scheme was devised to categorize the data into different degrees of cavitation based on the visual observations (table 1). The correlation between the non-deterministic energy and dp/dt was high for the Björk-Shiley and CarboMedics valve ($r^2 = 0.74$ *and* 0.99, *respectively*), but less satisfactory for the Medtronic Hall valve ($r^2 = 0.56$).

Hence, the non-deterministic signal energy seemed to be a better means of quantifying cavitation than visually grading, dp/dt, or the RMS parameter. Clearly, non-deterministic signal energy increased when visual cavitation increased. The two tilting disc valves had comparable non-deterministic energy, but the energy of the bileaflet CarboMedics valve was markedly lower. It was observed that this valve was more difficult in adjusting different degrees of cavitation. In theory, the bileaflet valves should cause less cavitation than the tilting disc valves, due to the smaller momentum of the bileaflet valve occluder. These data suggest that the CarboMedics valve is less likely to cause cavitation than the investigated tilting disc valves. Furthermore, the energy created during bubble collapse may be smaller than that observed at the tilting disc valves, even at the same dp/dt levels.

The presented non-deterministic energy method is suggested as an alternative analysis method for quantitative evaluation of cavitation to the formerly presented high-pass filter method [10]. A previous study has shown that using the high-pass filter method requires that the filter should be designed carefully due to differences in spectral characteristics for different individual valves

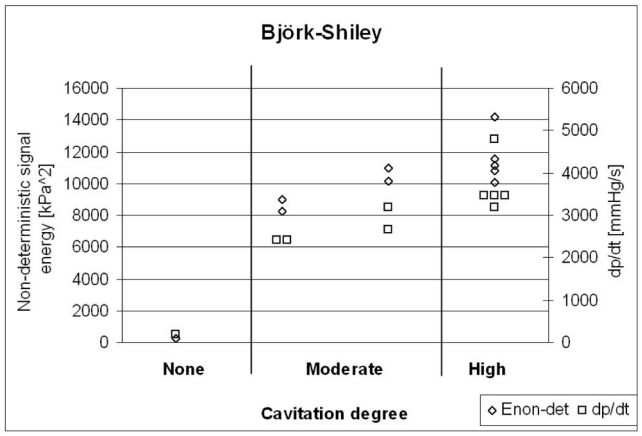

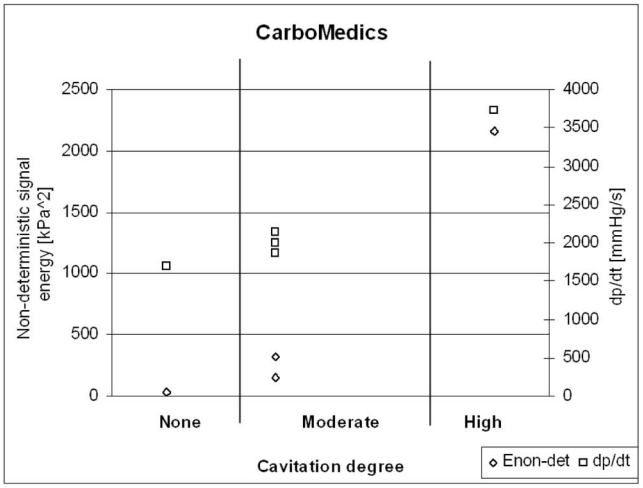

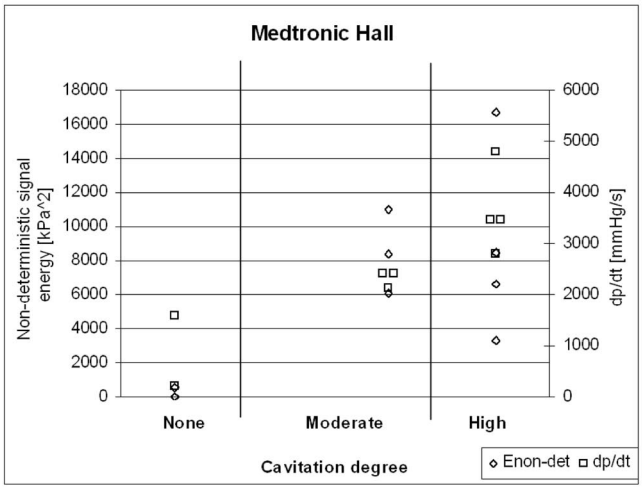

Fig. 5 The non-deterministic energy and *dp/dt* plotted as a function of the cavitation degree based on the visual criteria for the three valves investigated.

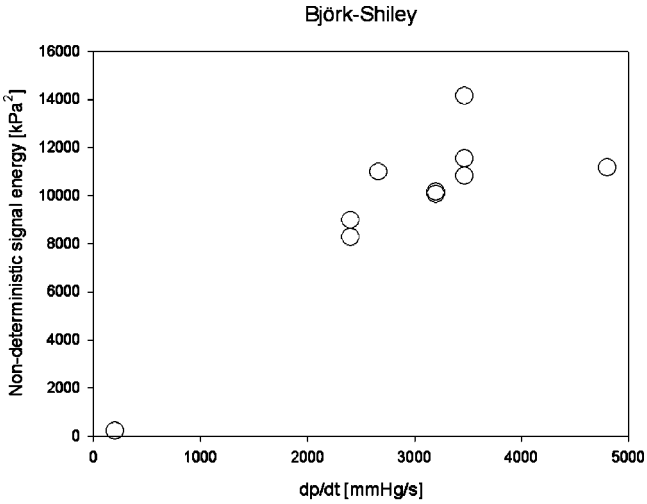

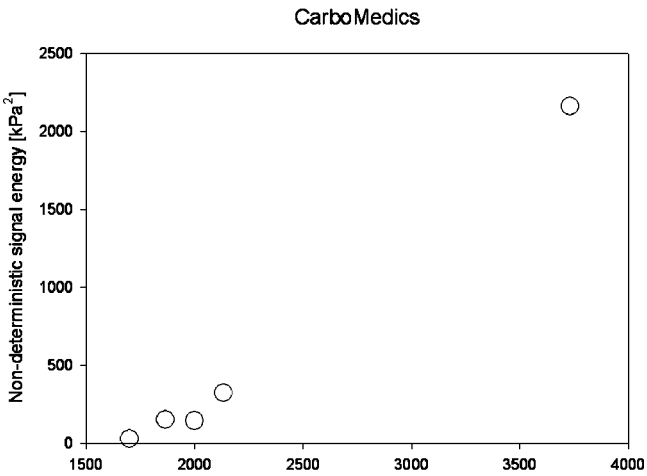

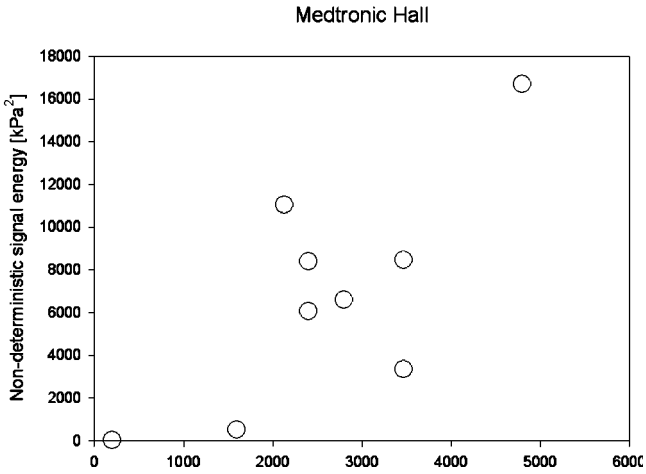

Fig. 6 The non-deterministic energy plotted as a function of *dp/dt* for the three valves. Björk-Shiley $r^2 = 0.74$; CarboMedics $r^2 = 0.99$: Medtronic Hall $r^2 = 0.56$.

[11]. Comparing the cavitation indexes of the RMS values derived from the high-pass filter method to the non-deterministic energy from the new method showed a very high correlation (Fig. 7). The RMS values were calculated based on the cut-off frequency for each valve proposed by Johansen et al.

However, the main advantage of the non-deterministic energy method is that it does not require *a priori* knowledge of the resonance pattern from the investigated valve in order to design the high-pass filter. Furthermore, it does not introduce bandwidth limitations of the cavitation signal as a consequence of filtering, and the method will be applicable *in vivo*.

Even though the new method has the advantage of not requiring *a priori* knowledge of the valve closing characteristics and there is no bandwidth limitation, it might not be optimal for analyzing bileaflet valves due to the asynchronous nature of the closing of these valve designs [20], causing signal component nonalignment

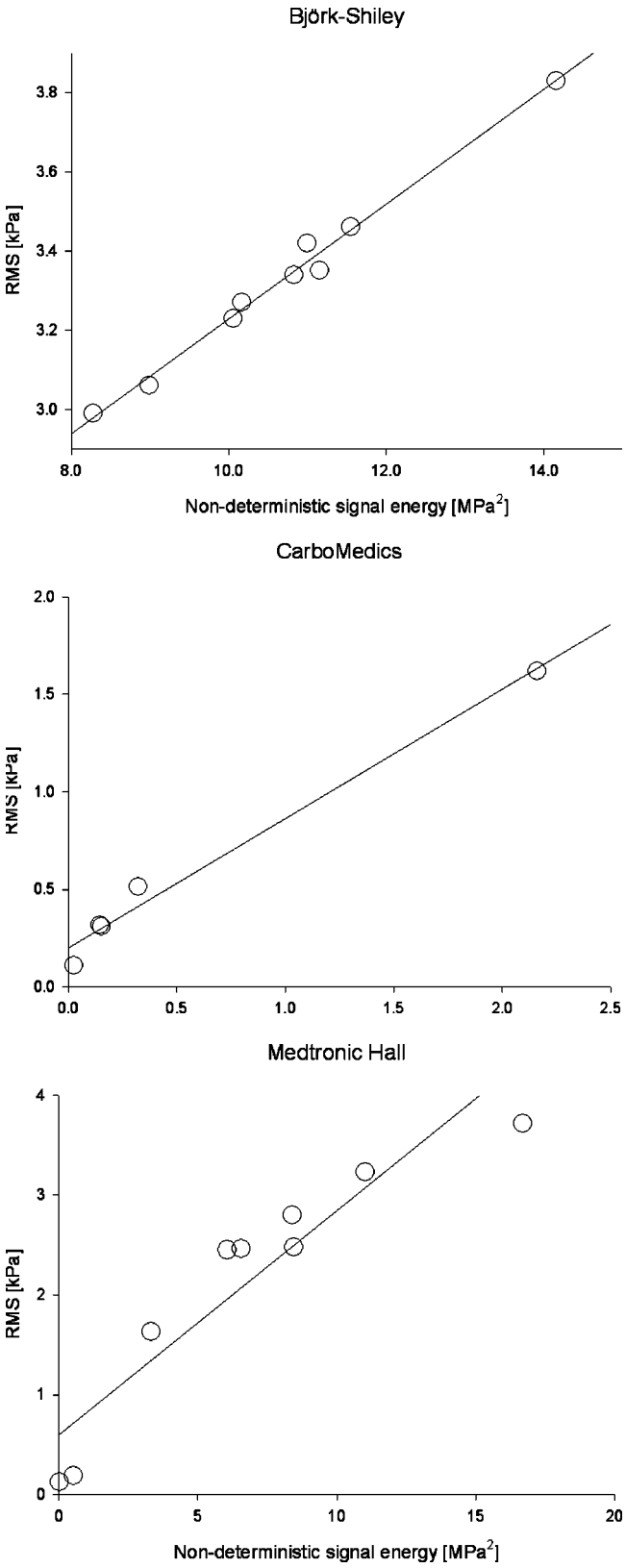

Fig. 7 The RMS value of the high-pass filtered pressure data is plotted as a function of non-deterministic energy for the three valves. The high-pass filter is designed based on a priori knowledge of the particular valve's mechanical resonance characteristic. Björk-Shiley valve $r^2=0.99$; CarboMedics valve $r^2=0.98$; Medtronic Hall valve $r^2=0.88$.

Table 2 The time between closures of the two leaflets at the CarboMedics valve is shown as a mean and standard deviation for four different hemodynamic situations (dp/dt).

dp/dt [mmHg/s]	Time between leaflet closures Mean ± std. dev. [ms]
1700	3.55 ± 0.56
1866	0.77 ± 0.26
2133	0.97 ± 0.13
2000	0.88 ± 0.44

before ensemble averaging. Additionally, this can introduce two impulse related signals separated by very short time, which might have different contents of deterministic and non-deterministic signal components. Further studies are needed in order to evaluate the applicability of this method to those valve types.

Study limitations

With the CarboMedics valve only five data points were acquired. With a predefined data acquisition scheme it was difficult to acquire a wide variety of different cavitation levels. Furthermore, the cavitation threshold limit seemed very fine, meaning that above a certain valve load limit the valve started to create pronounced cavitation. Thus, intermediate levels of cavitation were not acquired. The correlation coefficient calculated based on the CarboMedics data was determined by the isolated data point at high cavitation, and therefore has limited value.

Conclusion

It is possible to evaluate and quantify cavitation by isolating the non-deterministic part of the high-frequency pressure fluctuations that are generated at cavitating valve closure. This method has the advantage that it does not require *a priori* knowledge of the spectral characteristics for the investigated valves and it does not limit the bandwidth of the signal.

Acknowledgment

This study has kindly been financially supported by the National Heart Lung and Blood Institute grant RO1 HL48652, the Danish Heart Foundation grants 00-1-2-22-22792A and 00-1-2-22-22792B, and by Snedkermester Sophus Jacobsen og hustru Astrid Jacobsens Fond.

References

[1] Yoganathan, A. P., 2000, "Cardiac Valve Prostheses" *The Biomedical Engineering Handbook*, J. Bronzino, editor, CRC Press, Boca Raton, Florida, pp. 1847–1870.
[2] Knapp, R. T., Daily, J. W., and Hammitt, F. G., 1970, *Cavitation*, 1st edition, McGraw-Hill Book Co., New York, NY, pp. 321–357.
[3] Klepetko, W., et al., 1989, "Leaflet Fracture in Edwards-Duromedics Bileaflet Valves," J. Thorac. Cardiovasc. Surg., **97**(1), pp. 90–94.
[4] Graf, T., et al., 1991, "Cavitation Potential of Mechanical Heart-Valve Prostheses," Int. J. Artif. Organs, **14**(3), pp. 169–174.
[5] Kafesjian, R., et al., 1994, "Cavitation Damage of Pyrolytic Carbon in Mechanical Heart Valves," J. Heart Valve Dis., **3** (Suppl 1:S2–7(S2–S7)), pp. 2–7.
[6] Haubold, A. D., Ely, J. L., and Chahine, G. L., 1994, "Effect of cavitation on pyrolytic carbon in vitro.," J. Heart Valve Dis., **3**(3), pp. 318–323.
[7] Wu, Z. J., et al., 1994, "The Closing Behavior of Medtronic Hall Mechanical Heart Valves," ASAIO J., **40**(3), pp. M702–M706.
[8] Wu, Z. J., Gao, B. Z., and Hwang, N. H., 1995, "Transient Pressure at Closing of a Monoleaflet Mechanical Heart Valve Prosthesis: Mounting Compliance Effect," J. Heart Valve Dis., **4**(5), pp. 553–567.
[9] He, Z., et al., 2001, "Mechanisms of Mechanical Heart-Valve Cavitation: Investigation Using a Tilting Disk-Valve Model," J. Heart Valve Dis., **10**(5), pp. 666–674.
[10] Garrison, L. A., et al., 1994, "An In-Vitro Investigation of Prosthetic Heart-Valve Cavitation in Blood," J. Heart Valve Dis., **3** (Suppl 1:S8–22, discussion S22-4(S8–22)), pp. 8–24.

[11] Johansen, P., Lomholt, M., and Nygaard, H., 2002, ''Spectral Characteristics of Mechanical Heart-Valve Closing Sounds,'' J. Heart Valve Dis., **11**(5), pp. 736–744.
[12] Brennen, C. E., 1995, *Cavitation and Bubble Dynamics*, 1st edition, Oxford University Press, Inc., New York, NY, pp. 83–91.
[13] Oba, R., et al., 2002, ''Stochastic Behavior (Randomness) of Desinent Cavitation,'' J. Fluids Eng., **108**(4), pp. 438–443.
[14] Kini, V., et al., 2000, ''Flow Visualization in Mechanical Heart Valves: Occluder Rebound and Cavitation Potential,'' Ann. Biomed. Eng., **28**(4), pp. 431–441.
[15] Chandran, K. B., and Aluri, S., 1997, ''Mechanical Valve Closing Dynamics: Relationship Between Velocity of Closing, Pressure Transients, and Cavitation Initiation,'' Ann. Biomed. Eng., **25**(6), pp. 926–938.
[16] Wu, Z. J., Slonin, J. H., and Hwang, N. H., 1996, ''Transient Pressure Signals in Mechanical Heart-Valve Cavitation,'' ASAIO J., **42**(5), pp. M555–M561.
[17] Lee, C. S., Chandran, K. B., and Chen, L. D., 1996, ''Cavitation Dynamics of Medtronic Hall Mechanical Heart-Valve Prosthesis: Fluid Squeezing Effect,'' J. Biomech. Eng., **118**(1), pp. 97–105.
[18] Herman, B. A., and Carey, R. F., 1994, ''A Protocol for the Evaluation of the Cavitation Potential of Mechanical Heart Valves,'' J. Heart Valve Dis., **3** [Suppl 1:S128–30, discussion S130–2(S128–S130)], pp. 128–132.
[19] Dawson, B., and Trapp, R. G., 2001, *Basic & Clinical Biostatistics*, 3rd edition, McGraw-Hill Book Co., Singapore.
[20] Donnerstein, R. L., and Allen, H. D., 1990, ''Asynchronous Leaflet Closure in the Normally Functioning Bileaflet mechanical valve,'' Am. Heart J., **119**(3 Pt 1), pp. 694–697.
[21] Kingsbury, C., et al., 1993, ''Cavitation Threshold With Respect to dP/dt: Evaluation in 29 mm Bileaflet, Pyrolitic Carbon Heart Valves,'' Int. J. Artif. Organs, **16**(7), pp. 515–520.
[22] Shu, M. C., et al., 1994, ''In Vitro Observations of Mechanical Heart-Valve Cavitation,'' J. Heart Valve Dis., **3** [Suppl 1:S85–92, discussion S92–3(S85–S92)], pp. 85–93.